Desalination and Water Treatment
www.deswater.com

doi: 10.5004/dwt.2018.22762

127 (2018) 272–281
September

Kinetics, thermodynamics and isotherm parameters of uranium(VI) adsorption on natural and HDTMA-intercalated bentonite and zeolite

Adrián Krajňák[a,*], Eva Viglašová[a], Michal Galamboš[a,*], Lukáš Krivosudský[a,b]

[a]*Department of Inorganic Chemistry, Faculty of Natural Sciences, Comenius University in Bratislava, Mlynská Dolina, Ilkovičova 6, 842 15 Bratislava, Slovakia, Tel. +421 2 602 96 351; Fax: +421 2 602 96 273; emails: krajnak14@uniba.sk (A. Krajňák), michal.galambos@uniba.sk (M. Galamboš), eva.viglasova@uniba.sk (E. Viglašová), lukas.krivosudsky@univie.ac.at (L. Krivosudský)*
[b]*Department of Biophysical Chemistry, Faculty of Chemistry, University of Vienna, Althanstraße 14, 1090 Vienna, Austria*

Received 31 January 2018; Accepted 8 July 2018

ABSTRACT

The novelty of this work consists in the new organo-adsorbents development for anionic forms of uranium adsorption by bentonites and zeolites from Greek deposits with significant meaning. The main aim of this study was the comparison between Greek bentonite Kimolos and zeolite Metaxades, natural and organo-modified forms towards adsorption of U(VI) from aqueous solution. Chemical modification method with hexadecyltrimethylammonium bromide (HDTMABr) was used for organo-forms preparation. The effect of pH and contact time, as well as kinetic, isotherms and thermodynamic adsorption of U(VI) on studied bentonite and zeolite has been investigated by batch experiments and discussed by different mathematical models. The study indicates that prepared HDTMA forms can be potentially used as promising low-cost adsorbents for U(VI) removal in waste water treatment.

Keywords: Adsorption; Bentonite; Organobentonite; Zeolite; Organozeolite; Intercalation; HDTMA; Uranium

1. Introduction

Bentonites and zeolites are naturally occurring structured aluminosilicates, with high cation exchange and ion adsorption capacity [1–12]. Bentonite rocks consist mainly of montmorillonite (50%–80%), a mineral from dioctaedric smectite group; and accompanying materials such as clay mineral, quartz diatomite, calcite, organic materials and others [13–15]. Montmorillonite, a clay mineral with 2:1 layered structure, can hold some cations between its layers. Substitution of Si^{4+} with Al^{3+} in tetrahedral sheets and Al^{3+} with Mg^{2+} in octahedral sheets gives the lattice a net negative charge which is usually balanced by cations of Li^{+}, Na^{+} and Ca^{2+} located between the layers. These cations can easily be replaced by other organic or inorganic cations [16–18]. Zeolite is natural porous mineral described as crystalline hydrated aluminosilicate. Inside the framework structure of zeolite, alkali or alkaline-earth cations are reversibly fixed in the cavities and can easily be exchanged by surrounding positive ions [19–22]. Clinoptilolite belongs to the natural zeolite with high ion-exchange and adsorption properties and it is known to have high exchange capacity and removal efficiency for some cations [23,24]. Bentonites and zeolites have a high potential for natural and waste uranium management [25]. The removal and recovery of uranium from contaminated soils, environment and ground water, as a result of nuclear industry, has attracted more and more attention [26–32].

Uranium is the most abundant long-lived natural radionuclide ($T_{1/2}$ = 4.51 × 10^9 years for U-238) and is stable in many soil and aquifer systems. Uranium occurs as a mobile hydrated uranyl UO_2^{2+} ion and various soluble uranyl complexes under near surface conditions [33,34]. It is therefore a potentially hazardous pollutant to the environment.

Several methods are available for removing uranium from aqueous solution, such as electrodeposition, chemical

* Corresponding author.

precipitation, reverse osmosis, solvent extraction, micellar ultrafiltration and adsorption [35–42]. Among these, adsorption is the most attractive method, due to its high efficiency, ease of handling and availability of different adsorbents. Various kinds of new adsorbents for removing and recovering radionuclides including uranium have been reported, among which natural bentonites [43–46], zeolites [47–50] and their modified forms are considered as particularly effective, low-cost and chemically stable [51–58].

Natural bentonites and zeolites are unsuccessful for anions adsorption [59–65], thus the surface modification has been proposed to enhance the adsorption capacity for anions. The organo-silicates belong to the adsorbents obtained through replacement of mobile inorganic cations (such as Na^+), by the large hydrophobic quaternary alkylammonium in cationic form. Based on the modification, they are suitable to adsorb contaminants in anionic forms.

Herein, Greek natural bentonite from deposit Kimolos and zeolite from deposit Metaxades for U(VI) cationic species removal was studied. HDTMA-bentonite (KIm) and HDTMA-zeolite (MXm) were prepared in order to obtain more efficient adsorbent for U(VI) anionic species removal. The HDTMA-intercalated adsorbents were characterized by Fourier transform infrared (FTIR) spectroscopy and the batch technology was adopted to evaluate the adsorption capacity of KIm and MX towards U(VI) as a function of contact time, pH, initial U(VI) concentration and temperature. The adsorption kinetic, various isotherms and thermodynamics calculations of U(VI) were investigated.

2. Experimental

Herein, some crucial points of experimental conditions are explained and for more detailed description follow our previous, already published study [65].

2.1. Reagents

- Stock U(VI) solution: $UO_2(NO_3)_2 \cdot 6H_2O$ in distilled water,
- Buffer solutions (pH 4, 7 and 9): adjusted with 0.1 mol L^{-1} HCl and 0.1 mol L^{-1} NaOH,
- All reagents used during experiments were of analytical purity.

2.2. Natural and HDTMA forms

- Greek bentonite Kimolos: natural forms labelled KI, fractions below 15 μm, Specific surface area (SSA) ~ 680 $m^2 g^{-1}$, cation exchange capacity (CEC) 96 meq 100 g^{-1} [66,67].
- Greek zeolite Metaxades: natural forms labelled MX, fractions below 15 μm, SSA ~ 760 $m^2 g^{-1}$, CEC 119 meq 100 g^{-1} [66,67].
- HDTMA forms of bentonite was labelled KIm and zeolite was labelled MXm, fractions below 50 μm.
- The preparation of HDTMA intercalated forms: 5 g of KI or MX was mixed with 25 mL, 60 mmol L^{-1} HDTMABr solution and stirred at 60°C for 24 h.
- Followed by filtration and washed with deionized water until a negative bromide test with 0.1 mol L^{-1} $AgNO_3$ was obtained.
- Final suspension was dried at 60°C for 24 h.
- Tables 1–4 contain main characteristics and chemical compositions of the studied natural bentonite and zeolite.

2.3. Adsorption experiments

- Adsorption experiments were studied by batch technique.
- Adsorption of U(VI) was studied as a function of pH, contact time, initial U(VI) concentration and temperature.
- Equilibrium experiments: 0.05 g of adsorbent was suspended 24 h in 10 mL of the solution with various U(VI) concentration.
- Concentrations: 10, 50, 100, 250, 500, 750 and 1,000 ppm.
- Initial pH: 2.5, 3.0, 8.0, 8.5, 9.5 and 10.5.
- U(VI) concentrations were determined by UV-Vis Spectrophotometer (Shimadzu UV-Vis 160A) after adsorption in the solution by the Arsenazo III method.
- Amount of U(VI) ions adsorbed per unit mass of the adsorbent was calculated by using the following equation:

$$q_e = \frac{(c_0 - c_e)V}{m} \quad (1)$$

Table 1
The main characteristic of KI bentonite

Origin of the bentonite	Kimolos/Greece
Exchangeable cation	Na^+, Ca^{2+}
Bentonite type	Montmorillonite
Bentonite content	90%

Table 2
The chemical composition of KI bentonite (in wt%)

Bentonite	KI
SiO_2	35.94
Al_2O_3	12.78
CaO	0.02
K_2O	0.01
Na_2O	17.47
Fe_2O_3	1.05
MgO	2.12
MnO	0.01
TiO_2	0.09
P_2O_5	0.04
Cr_2O_3	0.002

Table 3
The main characteristic of MX zeolite

Origin of the zeolite	Metaxades/Greece
Exchangeable cations	Ca^{2+}, K^+
Zeolite type	HEU-type clinoptilolite
Zeolite content	58%

Table 4
The chemical composition of MX zeolite (in wt%)

Zeolite	MX
SiO_2	66.47
Al_2O_3	13.47
CaO	3.25
K_2O	2.6
Na_2O	2.09
Fe_2O_3	1.05
MgO	0.65
MnO	0.02
TiO_2	0.15
H_2O	10
Si/Al	4.93

where q_e is the adsorption capacity of the adsorbent (mg g^{-1}), c_0 and c_e are the initial and equilibrated U(VI) concentrations (mg L^{-1}) respectively, V is the volume of the aqueous solution (mL) and m is the mass of dry adsorbent material (mg).

- Kinetic experiments: 0.5 g of adsorbent was suspended in 100 mL solution, containing 500 ppm U(VI).
- Temperatures: 25°C, 35°C and 45°C.
- Initial pH: 2.5 and 8.5.
- The relative error of Arsenazo III determination does not exceed 4% [68].

3. Results and discussion

3.1. Characterization

The FTIR spectra of the adsorbents were recorded with a Shimadzu 8400S spectrometer in the wavelength range of 500–4,000 cm^{-1}. The IR spectrum of natural bentonite KI and HDTMA-bentonite KIm is shown in Fig. 1.

The position and shape of the –OH stretching band in the IR spectra of bentonite minerals are basically influenced by the nature of the octahedral atoms to which the hydroxyl groups are coordinated. A group of absorption peaks was observed between 3,620 and 3,404 cm^{-1}, which is due to –OH stretching vibration bands of the water in HDTMA-bentonite and their bending vibrations at 910 and 917 cm^{-1}, which is consistent with other studies. The absorption band at 3,620 cm^{-1}, found in the spectrum is typical for smectite minerals with large amounts of Al in the octahedral sheets. Another band at around 3,404 cm^{-1} (stretching vibration of the –OH groups) was observed. Asymmetric and symmetric C–H stretching vibrations of the $(–CH_2)_n$ groups in the HDTMA carbon chains on the HDTMA-bentonite are represented by bands at 2,936–2,873 cm^{-1}. The band of a bending vibration at 1,466 cm^{-1} is ascribed to the deformation of $–CH_2$, which is also observed in the HDTMA-bentonite. This supports the modification of bentonite adsorbents with surfactant cations. The observed bands at 1,649 cm^{-1} in intercalated bentonite, also correspond to the –OH deformation of water [69,70].

The IR spectrum of natural zeolite MX and HDTMA-zeolite MXm is shown in Fig. 2. The strongest bands are found in the range 950–1,250 cm^{-1}, which are assigned to the T–O stretching vibrations (T = Si or Al). The band of hydroxyl –OH vibration appears near 3,550 cm^{-1} in the spectrum indicating the bimodal absorbance. The water molecules attached to zeolite framework show strong characteristic structure sensitive bands due to water (H_2O) bending vibration at 1,630 cm^{-1}. The peaks between 700 and 850 cm^{-1} are assigned to symmetric and antisymmetric T–O–T stretching vibration. Asymmetric and symmetric C–H stretching vibrations of the $(–CH_2)_n$ groups in the HDTMA carbon chains on the HDTMA-zeolite are represented by bands at 2,917–2,833 cm^{-1}. The band of a bending vibration at 1,393 cm^{-1} was assigned to vibration of trimethylammonium quaternary group $CN(CH_3)_3^+$ [71–73].

3.2. Influence of pH

The adsorption behaviour of the functionalized groups of adsorbents towards metal ion removal depends on the protonation and deprotonation properties of its acidic and basic groups. The species distribution of uranyl ions in aqueous

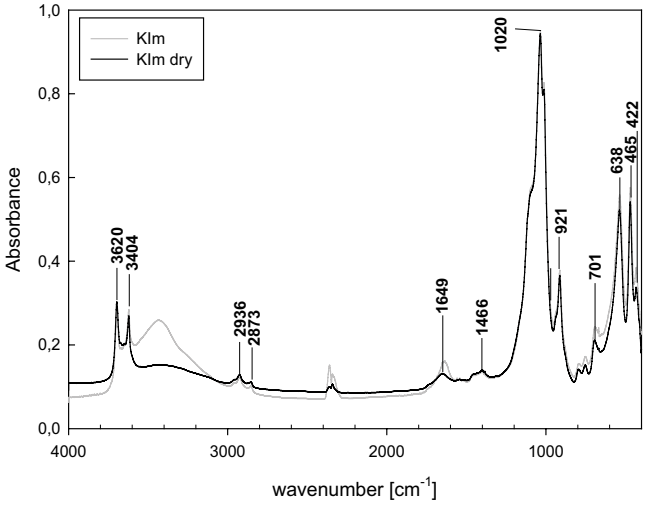

Fig. 1. FTIR spectra of KIm HDTMA-bentonite.

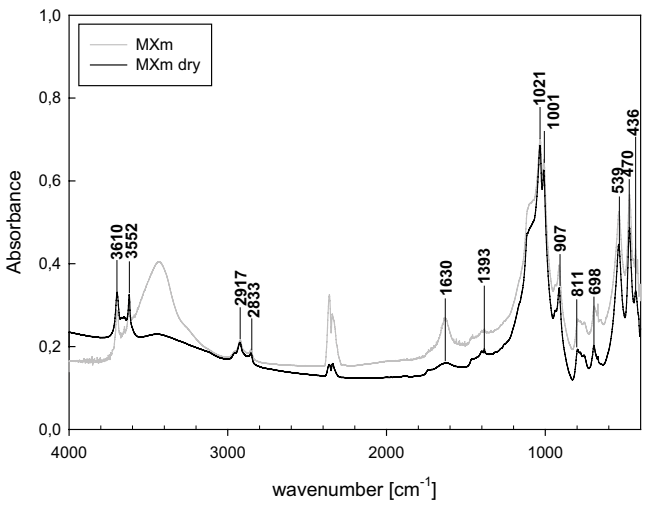

Fig. 2. FTIR spectra of MXm HDTMA-zeolite.

solution, influenced by pH, was described by Pourbaix diagram [74]. As the diagram shows, uranyl in cationic form (UO_2^{2+}) represents more than 95% of the U(VI) species in solution at pH < 4.0. There have been done many works even with the lower pH in the case of montmorillonite and clinoptilolite, but they conclude the destruction of structure, under the pH 2.0 [75]. Based on our previous experiences [65], we started experiment at pH_{init} = 2.5. The pH values were measured (Table 5) and compared after 24 h of mixing the solid/liquid phase, where the precipitation was not observed. The yellow precipitation occurs at pH above 6, where U(VI) is in the form of $UO_2(OH)_2$. The change of pH is also influenced by natural pH of bentonite and zeolite presented in aqueous solutions [65].

Fig. 3 shows the results of experiments with HDTMA-bentonite and HDTMA-zeolite, performed in the pH range 8.5–10.5. At higher pH (>7.5) U(VI) is in the solution distributed in anionic forms, carbonatodioxidouranate complexes $[UO_2(CO_3)_2]^{2-}$ and $[UO_2(CO_3)_3]^{4-}$ [74]. Solutions of U(VI) carbonato-complexes were prepared by adjusting the stock U(VI) solution to alkaline pH, continuously with mechanical stirring of solution (90 min, 25 rpm) and resulted in a natural uptake of CO_2 to the solutions from air.

Initial pH of experiments with HDTMA-bentonite and HDTMA-zeolite was determined at pH_{init} = 8.5. The pH values were measured (Table 5), compared after 24 h of mixing the solid/liquid phase and precipitation effect was not observed (Table 5).

During further experiments at pH = 9.5 and 10.5, we observed that lower initial U(VI) concentration resulted in the significantly higher pH_{equil}, in comparison with the pH_{init} due to the removal of OH^- ions by adsorbent.

The maximum adsorption capacity was reached at pH 9.5 for both studied HDTMA-intercalated forms (30.79 mg g^{-1} for KIm and 48.74 mg g^{-1} for MXm). At pH 10.5, there already was a significant decrease of adsorption (18.07 mg g^{-1} for KIm and 36.16 mg g^{-1} for MXm). Decrease of adsorption capacity at high pH could be explained by the adsorption of OH^- ions and spherical properties of competitive ions [65]. In the case of pH 8.5, it was not possible to evaluate the maximum adsorption capacity, because there was a precipitation at higher concentration for both HDTMA-intercalated forms. For this reason, following experiments were performed at pH = 9.5.

3.3. Influence of contact time

Fig. 4 shows the effect of contact time on U(VI) adsorption on studied adsorbents KI, KIm, MX and MXm. In all cases, we observed that the amount of adsorbed U(VI) sharply increased at the beginning and after 90 min the equilibrium was gradually reached. In the case of bentonite KI in the first 2 min ca. 60% of maximum uptake was observed, in comparison with the KIm, where it was just about 5% of maximum uptake in the first 2 min. On the other hand, zeolite MX in the first 2 min exhibited ca. 40% of maximum uptake, in comparison with the MXm, where it was just about 10% of maximum uptake. The faster adsorption rate at the beginning may be due to the availability of the active uncovered surface sides of the adsorbents [76]. Thus, the contact time 90 min was selected to establish adsorption equilibrium and used in all subsequent experiments. In both cases, the increase of temperature caused increase of adsorption ability of studied adsorbents.

3.4. Adsorption isotherm

To analyse the adsorption mechanisms, the adsorption isotherms of U(VI) on natural bentonite KI, natural zeolite MX and their HDTMA forms KIm and MXm at 298 K were investigated. Fig. 5 illustrates initial concentration effect on U(VI) adsorption. In addition, three traditional isotherms, that is, Langmuir [77], Freundlich [78] and Dubinin–Radushkevich (D-R) [79] models, were used to simulate the experimental data. Table 6 summarizes adsorption constants evaluated from the applied adsorption isotherms models with the correlation coefficients (R^2). Obtained results proved that the Langmuir isotherm model fitted best with the experimental data for description of the U(VI) adsorption process on studied adsorbent, based on the values of R^2. For further experiments (kinetics, thermodynamics), we were just based on Langmuir isotherm model. No calculations based on Freundlich and D-R models were performed, nor were they compared with the results of the Langmuir model.

3.5. Adsorption kinetics

The parameters of kinetic adsorption data were fitted by two typical pseudo-first-order and pseudo-second-order rate models, which are expressed as:

Table 5
Values of pH after 24 h of mixing the solid/liquid phases

Sample	pH_{init}	pH						
	c_{init} (ppm)	10	50	100	250	500	750	1,000
KI	2.5	2.98	2.85	2.79	2.73	2.72	2.68	2.62
MX		2.70	2.66	2.65	2.68	2.63	2.64	2.60
KIm	8.5	7.81	7.68	7.75	7.54	7.41	7.30	7.35
MXm		7.98	7.99	8.00	8.02	7.90	7.87	7.75
KIm	9.5	9.13	8.98	9.15	8.79	8.65	8.70	8.66
MXm		9.11	8.73	8.76	8.62	8.63	8.69	8.60
KIm	10.5	10.17	10.15	10.20	10.05	9.99	10.05	10.03
MXm		10.26	9.93	9.99	10.10	10.19	10.22	10.28

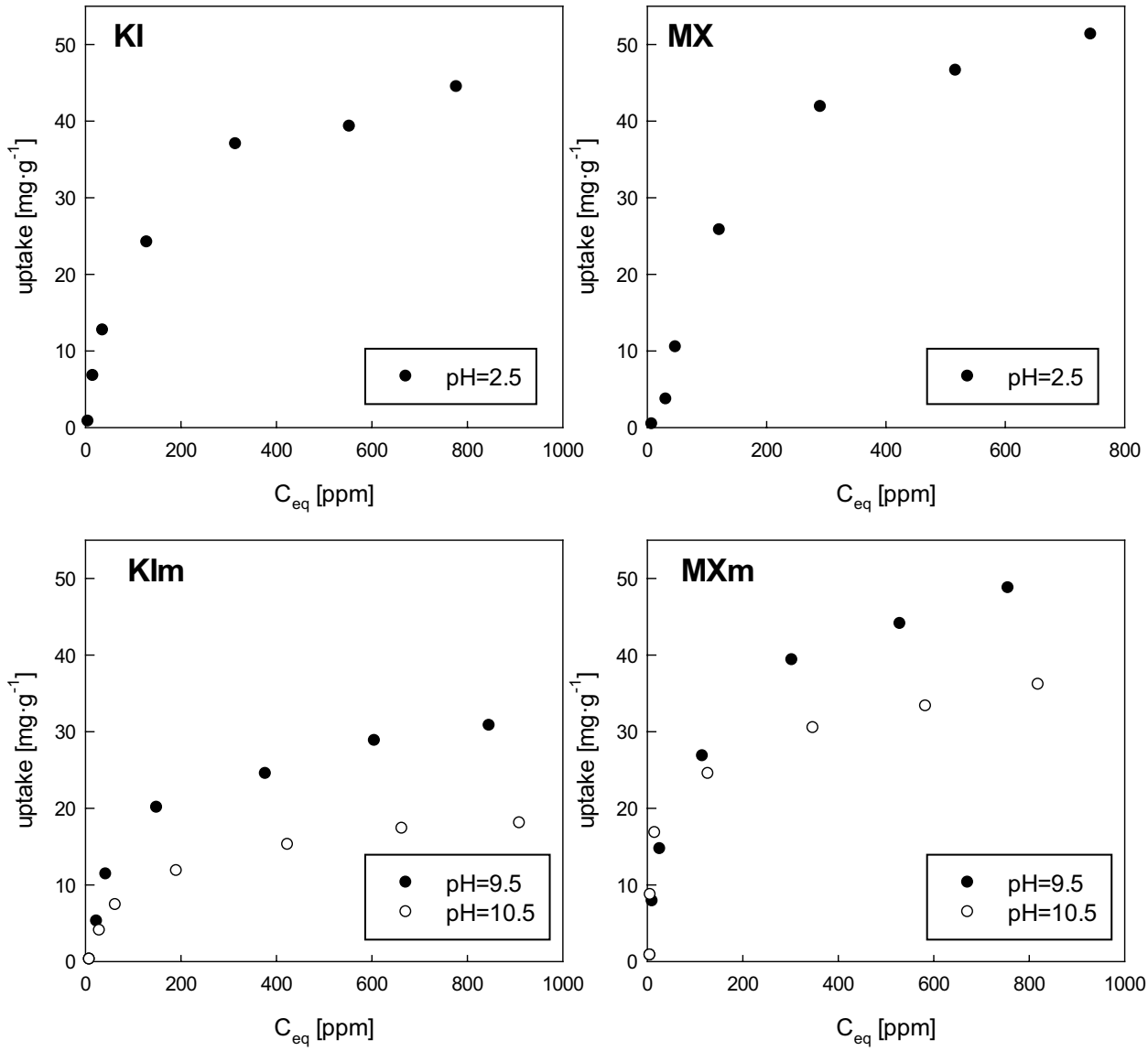

Fig. 3. The effect of pH on the adsorption of U(VI) on natural bentonite KI, zeolite MX and their HDTMA forms KIm, MXm at 298 K.

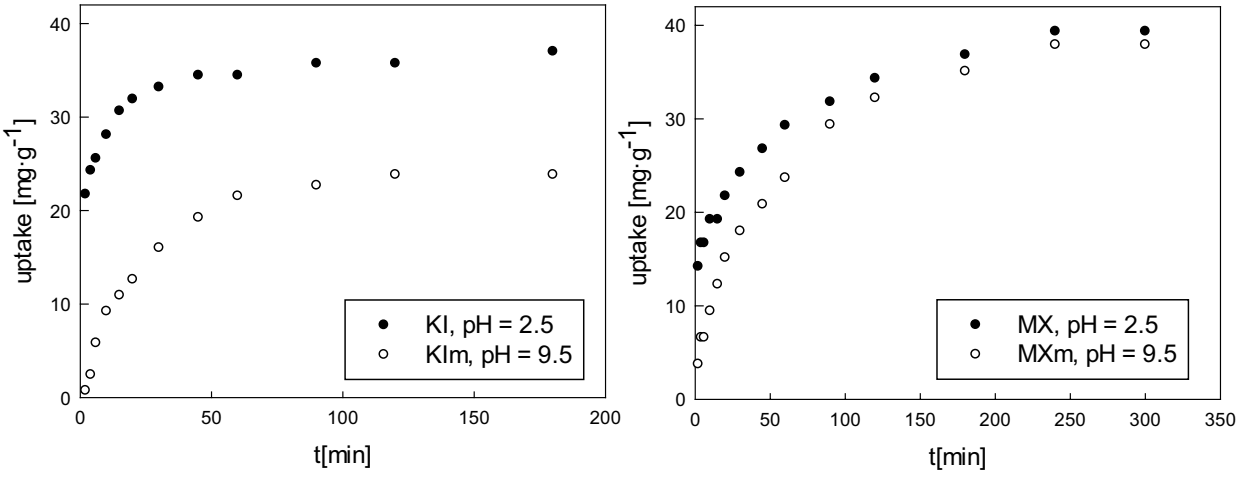

Fig. 4. The effect of contact time on U(VI) adsorption.

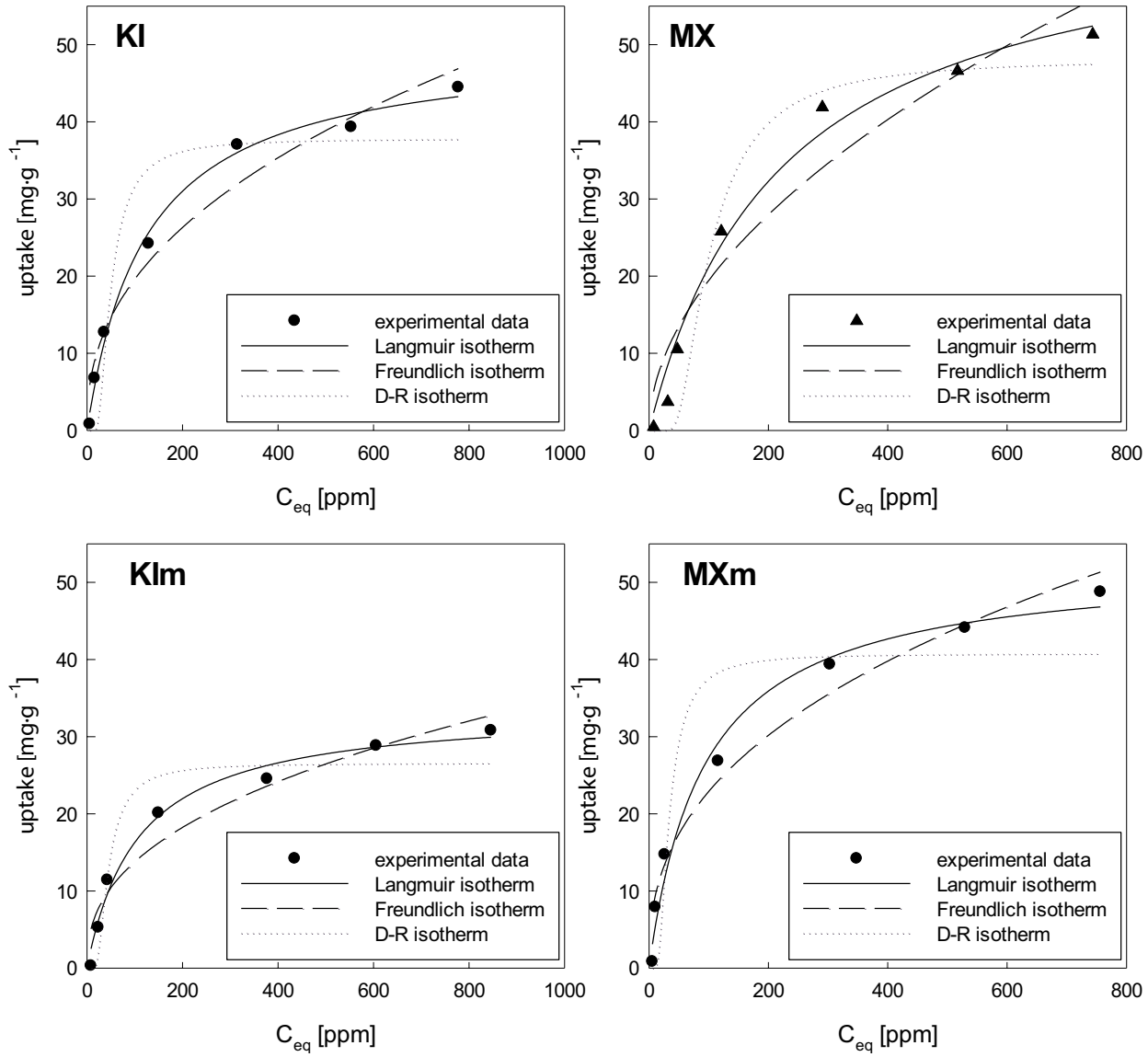

Fig. 5. The nonlinear form of adsorption isotherms of U(VI) on natural bentonite KI, zeolite MX and their HDTMA forms.

Table 6
Comparison of isotherm parameters of used models

Sample	Freundlich		Langmuir		D-R	
	K_F	R^2	Q_0	R^2	K_{AD}	R^2
KI	2.7502	0.9607	50.1279	0.9932	0.7146	0.8898
MX	1.7131	0.9351	68.04	0.9835	3.0448	0.9562
KIm	2.1187	0.9391	33.7091	0.9849	0.7146	0.8699
MXm	3.6288	0.9651	52.5687	0.9853	0.3333	0.5833

Pseudo-first-order model (Fig. 6) by Lagergren [80] is as follows:

$$\ln\left(q_e - q_t\right) = \ln q_e - k_1 t \tag{2}$$

Pseudo-second-order model (Fig. 7) by Ho [81] is as follows:

$$\frac{t}{q_t} = \frac{1}{k_2 q_e^2} + \frac{t}{q_e} \tag{3}$$

where q_e (mg g^{-1}) is the amount of U(VI) adsorbed on the adsorbents after adsorption equilibration, q_t (mg g^{-1}) is the amount of U(VI) adsorbed on the adsorbents at contact time t (h). k_1 (h^{-1}) is the pseudo-first-order kinetic constant which is obtained from linear fitting model. k_2 (mg g^{-1} h^{-1}) is the pseudo-second-order kinetic constant.

The kinetic parameters were calculated from the fitting models (Fig. 6) and were presented in Table 7. The correlation coefficient values (R^2) of pseudo-second-order model were higher and closer to the experimental data. Therefore, is possible to conclude that the adsorption process is more favourable with the pseudo-second-order equation, which indicated that adsorption process involves chemical reaction during adsorption in addition to physical adsorption [82].

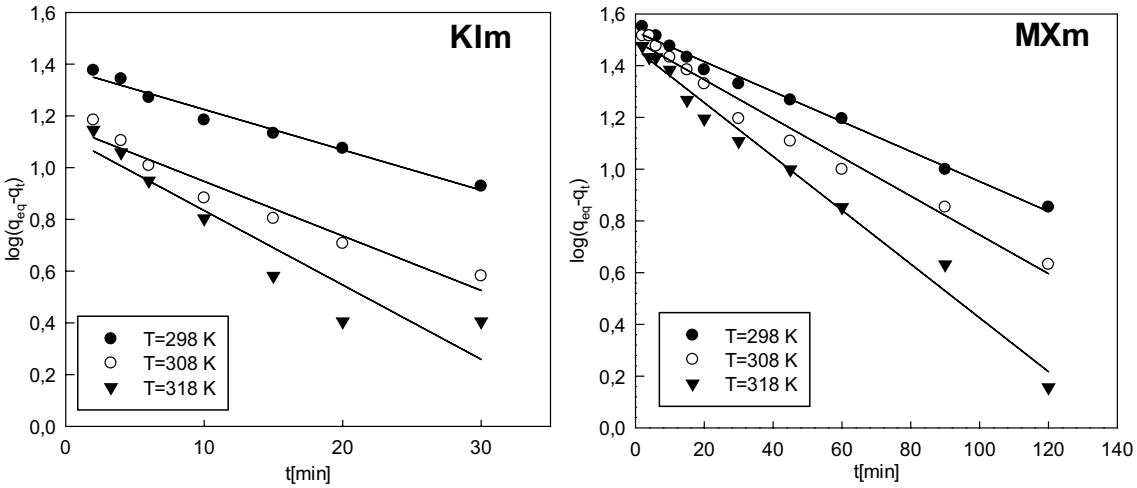

Fig. 6. The pseudo-first-order adsorption kinetics of U(VI) on KIm, MXm at pH = 9.5.

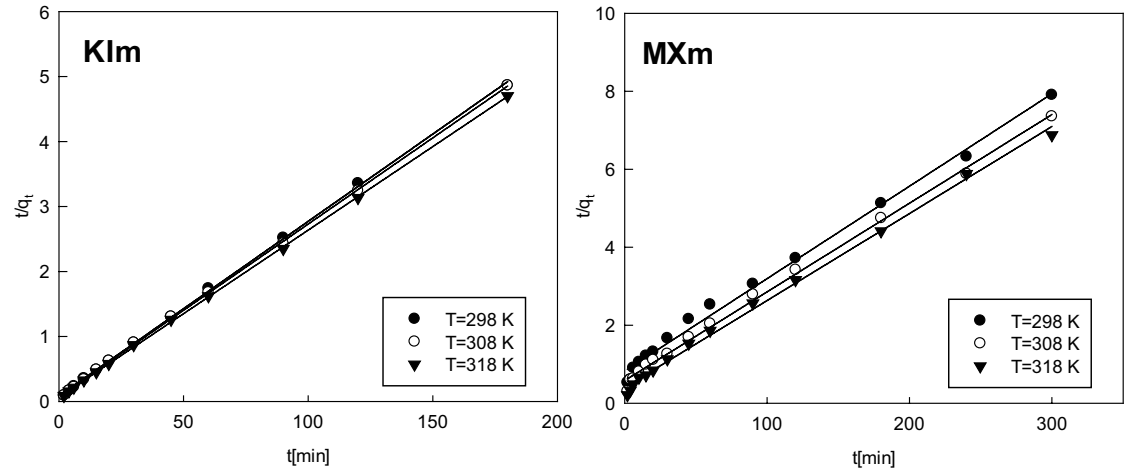

Fig. 7. The pseudo-second-order adsorption kinetics of U(VI) on KIm, MXm at pH = 9.5.

Table 7
Comparison of selected parameter from pseudo-first and pseudo-second order for the U(VI) adsorption

Sample	Pseudo-first order					Pseudo-second order		
	T (K)	$q_{e,\,exp}$ (mg g^{-1})	R^2	$q_{e,\,cal}$ (mg g^{-1})	k_1 (min^{-1})	R^2	$q_{e,\,cal}$ (mg g^{-1})	k_2 (g mg^{-1} min^{-1})
KI	298	37.17	0.9539	4.63	0.0184	0.9995	32.85	0.01975
	308	37.59	0.9653	4.78	0.0233	0.9997	32.52	0.02570
	318	38.91	0.9977	4.86	0.0684	0.9998	32.59	0.02395
MX	298	39.37	0.9853	4.75	0.0292	0.9943	33.99	0.01385
	308	41.89	0.9875	4.59	0.0200	0.9947	34.13	0.01549
	318	44.40	0.9748	4.76	0.0331	0.9977	34.60	0.01931
KIm	298	29.94	0.9750	22.38	0.0143	0.9995	21.62	0.00262
	308	27.40	0.9441	22.89	0.0223	0.9998	21.88	0.00282
	318	26.74	0.8864	22.71	0.0253	0.9997	23.40	0.00314
MXm	298	37.94	0.9924	29.89	0.0129	0.9935	31.14	0.00272
	308	40.78	0.9799	28.57	0.0151	0.9966	31.28	0.00253
	318	43.63	0.9853	31.90	0.0143	0.9964	33.35	0.00332

3.6. Adsorption thermodynamics

Activation energy is an important factor for determining the reaction rate. Activation energy of the U(VI) adsorption was calculated using linear form of Arrhenius equation, Eq. (4) [83].

$$\ln k = -\frac{E_a}{RT} + \ln A \quad (4)$$

where k is rate constant for sorption (g mg^{-1} min^{-1}), A is Arrhenius constant (g mg^{-1} min^{-1}), E_a is activation energy (kJ mol^{-1}), R is universal gas constant (8.314 J mol^{-1} K^{-1}) and T is temperature (K).

The values of the constant rate were calculated from the pseudo-second-order kinetic equation at three different temperatures: 298, 308 and 318 K. The values of E_a from the Arrhenius plots for natural adsorbents KI and MX are 2.113 and 2.738 kJ mol^{-1}, for HDTMA forms KIm and MXm are 49.674 and 17.220 kJ mol^{-1}, respectively. The calculated values of E_a indicate that the removal of U(VI) occurred through physical adsorption process. Higher E_a values of HDTMA forms indicate the endothermic behaviour during adsorption reaction of U(VI) ions. It is explained by large amount of heat consumption for carbonatodioxidouranate complexes transport from aqueous into the solid phase [65].

4. Conclusions

The novelty of this work consists in the new organo-adsorbents development for anionic forms of uranium adsorption by bentonites and zeolites from Greek deposits with significant meaning. The Greek natural adsorbents bentonite Kimolos, zeolite Metaxades were used for HDTMA-intercalated adsorbents preparation. The HDTMA forms were prepared by ion exchange process. Structure of the HDTMA forms was proved by FTIR analysis. The maximum adsorption capacity of HDTMA forms was obtained at pH 9.5 after 90 min of contact time. The U(VI) adsorption on natural- and HDTMA forms fitted better the Langmuir adsorption isotherm and pseudo-second-order kinetics models and the activation energy was calculated to 49,674 kJ mol^{-1} (KIm) and 17,220 kJ mol^{-1}(MXm), respectively. Zeolite Metaxades proved in both cases better removal efficiency, towards uranium-cationic species and HDTMA form for anionic species, respectively, in comparison with bentonite Kimolos. On the other hand, the kinetic of adsorption is faster in both the cases of bentonite Kimolos. However, bentonite and zeolite are two different adsorbents, both have good adsorption ability and they can be used in the field of waste management for uranium species removal from aqueous media.

Acknowledgements

This work was supported by the Grant Slovak Research and Development Agency APVV project no. SK-AT-2015-0003 and Agency of the Ministry of Education, Science, Research and Sport of the Slovak Republic and Slovak Academy of Sciences VEGA project no. 1/0507/17. The authors are grateful to the team of Department of Inorganic Chemistry, Aristotle University in Thessaloniki, Greece for professional help and valuable advices.

References

[1] M. Galamboš, P. Suchánek, O. Rosskopfová, Sorption of anthropogenic radionuclides on natural and synthetic inorganic sorbents, J. Radioanal. Nucl. Chem., 293 (2012) 613–633.
[2] R. Adamcová, F.T. Madsen, Heavy metal retardation in some Slovak clays and clayey soils, Geol. Carpathica Clays, 5 (1996) 13–20.
[3] K. Jablonská, I. Štyriaková, Application possibility of bentonite and zeolite in bioremediation, Adv. Mater. Res., 20–21 (2007) 295–298.
[4] B. Yıldız, H.N. Erten, M. Kış, The sorption behavior of Cs^+ ion on clay minerals and zeolite in radioactive waste management: sorption kinetics and thermodynamics, J. Radioanal. Nucl. Chem., 288 (2011) 475–483.
[5] E. Chmielewská, Zeolitic adsorption in course of pollutants mitigation and environmental control, J. Radioanal. Nucl. Chem., 299 (2014) 255–260.
[6] L. Chang-Han, P. Jeong-Min, L. Min-Gyu, Adsorption characteristics of Sr(II) and Cs(I) ions by zeolite synthesized from coal fly ash, J. Environ. Sci. Int., 23 (2014) 1987–1988.
[7] Z. Melichová, A. Ľuptáková, Removing lead from aqueous solutions using different low-cost abundant adsorbents, Desal. Wat. Treat., 57 (2016) 5025–5034.
[8] S. Inan, R. Koivula, R. Harjula, Removal of ^{63}Ni and ^{57}Co from aqueous solution using antimony doped tin dioxide-polyacrylonitrile (Sb doped SnO_2-PAN) composite ion-exchangers, J. Radioanal. Nucl. Chem., 299 (2014) 901–908.
[9] S. Inan, Y. Altas, Adsorption of strontium from acidic waste solution by Mn-Zr mixed hydrous oxide prepared by co-precipitation, Sep. Sci. Technol., 45 (2010) 269–276.
[10] V.N. Narwade, R.S. Khairnar, V. Kokol, In-situ synthesised hydroxyapatite loaded films based on cellulose nanofibrils for phenol removal from wastewater, Cellulose, 24 (2017) 4911–4925.
[11] V.N. Narwade, R.S. Khairnar, V. Kokol, In situ synthesized hydroxyapatite-cellulose nanofibrils as biosorbents for heavy metal ions removal, J. Polym. Environ., 7 (2017) 1–12.
[12] V.N. Narwade, R.S. Khairnar, Cobalt adsorption on the nano-hydroxyapatite matrix: isotherm and kinetic studies, Bull. Pol. Acad. Sci. Tech. Sci., 65 (2017) 131–137.
[13] Z. Danková, A. Mockovčiaková, S. Dolinská, Influence of ultrasound irradiation on cadmium cations adsorption by montmorillonite, Desal. Wat. Treat., 52 (2014) 5462–5469.
[14] Z Melichová, M. Handzušová, Removal of Cu(II) ions from aqueous solutions by adsorption onto natural bentonites, Solid State Phenom., 244 (2016) 205–212.
[15] M. Galamboš, O. Rosskopfová, J. Kufčáková, P. Rajec, Utilization of Slovak bentonites in deposition of high-level radioactive waste and spent nuclear fuel, J. Radioanal. Nucl. Chem., 288 (2011) 765–777.
[16] Y. Li, L. Zeng, Y. Zhou, T. Wang, Y. Zhang, Preparation and characterization of montmorillonite intercalation compounds with quaternary ammonium surfactant: adsorption effect of zearalenone, J. Nanomater., 2014 (2014) 7 pages, doi: 10.1155/2014/167402.
[17] A. Mockovčiaková, Z. Orolínová, J. Škvarla, Enhancement of the bentonite properties, J. Hazard. Mater., 180 (2010) 274–281.
[18] R. Zhang, Ch. Chen, J. Li, X. Wang, Preparation of montmorillonite-carbon composite and its application for U(VI) removal from aqueous solution, Appl. Surf. Sci., 349 (2015) 129–137.
[19] D. Wen, Y.S. Ho, Y. Tang, Comparative sorption kinetic studies of ammonium onto zeolite, J. Hazard. Mater., 133 (2005) 252–256.
[20] E. Chmielewská, J. Lesný, Selective ion exchange onto Slovakian natural zeolites in aqueous solutions, J. Radioanal. Nucl. Chem., 293 (2012) 535–543.

[21] M. Delkash, B.E. Bakhshayesh, H. Kazemian, Using zeolitic adsorbents to cleanup special wastewater streams: a review, Microporous Mesoporous Mater., 214 (2015) 224–241.
[22] T. Kobayashi, M. Ohshiro, K. Nakamoto, S. Uchida, Decontamination of extra-diluted radioactive cesium in Fukushima water using zeolite−polymer composite fibers, Ind. Eng. Chem. Res., 55 (2016) 6996–7002.
[23] A. Kilincarslan, S. Akyil, Uranium adsorption characteristic and thermodynamic behavior of clinoptilolite zeolite, J. Radioanal. Nucl. Chem., 24 (2005) 541–548.
[24] P. Rajec, K. Domianová, Cesium exchange reaction on natural and modified clinoptilolite zeolites, J. Radioanal. Nucl. Chem., 275 (2007) 503–508.
[25] A.L. Iskander, E.M. Khald, A.S. Sheta, Zinc and manganese sorption behavior by natural zeolite and bentonite, Ann. Agric. Sci., 56 (2011) 43–48.
[26] J. Liu, Ch. Zhao, H. Tu, J. Yang, F. Li, D. Li, J. Liao, Y. Yang, J. Tang, N. Liu, U(VI) adsorption onto cetyltrimethylammonium bromide modified bentonite in the presence of U(VI)-CO_3 complexes, Appl. Clay Sci., 135 (2017) 64–74.
[27] Q. Zuo, X. Gao, J. Yang, P. Zhang, G. Chen, Y. Li, K Shi, W. Wu, Investigation on the thermal activation of montmorillonite and its application for the removal of U(VI) in aqueous solution, J. Taiwan Inst. Chem. Eng., 80 (2017) 754–760.
[28] D. Baybas, Polyacrylamide–hydroxyapatite composite: preparation, characterization and adsorptive features for uranium and thorium, J. Solid State Chem., 194 (2012) 1–8.
[29] K. Popa, Sorption of uranium on lead hydroxyapatite, J. Radioanal. Nucl. Chem., 298 (2013) 1527–1532.
[30] S.S. Kim, G.N. Kim, U.R. Park, J.K. Moon, Development of a practical decontamination procedure for uranium-contaminated concrete waste, J. Radioanal. Nucl. Chem., 302 (2014) 611–616.
[31] P. Cakir, S. Inan, Y. Altas, Investigation of strontium and uranium sorption onto zirconium-antimony oxide/polyacrylonitrile (Zr-Sb oxide/PAN) composite using experimental design, J. Hazard. Mater., 271 (2014) 108–119.
[32] V. Guimaraes, E. Rodriguez-Castellon, M. Algarra, F. Rocha, I. Bobos, Kinetics of uranyl ions sorption on heterogeneous smectite structure at pH 4 and 6 using a continuous stirred flow-through reactor, Appl. Clay Sci., 134 (2016) 71–82.
[33] R. Atta-Fynn, D.F. Johnson, E.J. Bylaska, E.J. Ilton, G.K. Schenter, W.A. de Jong, Structure and hydrolysis of the U(IV), U(V), and U(VI) aqua ions from ab initio molecular simulations, Inorg. Chem., 51 (2012) 3016–3024.
[34] J. Kony, N.M. Nagy, Nuclear and Radiochemistry, Elsevier, Oxford, 2012.
[35] B.Q. Lu, M. Li, X.W. Zhang, C.M. Huang, X.Y. Wu, Q. Fan, Immobilization of uranium into magnetite from aqueous solution by electrodepositing approach, J. Hazard. Mater., 343 (2018) 255–265.
[36] C.A. Barrett, W. Chouyyok, R.J. Speakman, K.B. Olsen, R.S. Addleman, Rapid extraction and assay of uranium from environmental surface samples, Talanta, 173 (2017) 69–78.
[37] P. Singhal, S.K. Jha, S.P. Pandey, S. Neogy, Rapid extraction of uranium from sea water using Fe_3O_4 and humic acid coated Fe_3O_4 nanoparticles, J. Hazard. Mater., 335 (2017) 152–161.
[38] C. Cojocaru, G. Zakrzewska-Trznadel, A. Jaworska, Removal of cobalt ions from aqueous solutions by polymer assisted ultrafiltration using experimental design approach. Part 1: Optimization of complexation conditions, J. Hazard. Mater., 169 (2009) 599–609.
[39] Y. Zheng-ji, Y. Jun, C. Hui-lun, W. Fei, Y. Zhi-min, L. Xing, Uranium biosorption from aqueous solution onto *Eichhornia crassipes*, J. Environ. Radioact., 154 (2016) 43–51.
[40] S.S. Kim, G.S. Han, G.N. Kim, D.S. Koo, I.G. Kim, J.W. Choi, Advanced remediation of uranium-contaminated soil, J. Environ. Radioact., 164 (2016) 239–244.
[41] Z. Djedidi, M. Bouda, M.A. Souissi, R.B. Cheikh, G. Mercier, R.D. Tyagi, J.F. Blais, Metals removal from soil, fly ash and sewage sludge leachates by precipitation and dewatering properties of the generated sludge, J. Hazard. Mater., 172 (2009) 1372–1382.
[42] N. Kumari, D.R. Prabhu, P.N. Pathak, A.S. Kanekar, V.K. Manchanda, Extraction studies of uranium into a third-phase of thorium nitrate employing tributyl phosphate and N,N-dihexyl octanamide as extractants in different diluents, J. Radioanal. Nucl. Chem., 289 (2011) 835–843.
[43] F. Houhoune, D. Nibou, S. Chegrouche, S. Menacer, Behaviour of modified hexadecyltrimethylammonium bromide bentonite toward uranium species, J. Environ. Chem. Eng., 4 (2016) 3459–3467.
[44] J. Wang, Z. Chen, D. Shao, Y. Li, Z. Xu, C. Cheng, A.M. Asiri, H.M. Marwani, S. Hu, Adsorption of U(VI) on bentonite in simulation environmental conditions, J. Mol. Liq., 242 (2017) 678–684.
[45] P. Zong, X. Wu, J. Gou, X. Lei, D. Liu, H. Deng, Immobilization and recovery of uranium(VI) using Na-bentonite from aqueous medium: equilibrium, kinetics and thermodynamics studies, J. Mol. Liq., 209 (2015) 358–366.
[46] W. Yao, X. Wang, Y. Liang, S. Yu, P. Gu, Y. Sun, C. Xu, J. Chen, T. Hayat, A. Alsaedi, XK. Wang, Synthesis of novel flower-like layered double oxides/carbon dots nanocomposites for U(VI) and ^{241}Am(III) efficient removal: batch and EXAFS studies, Chem. Eng. J., 332 (2018) 775–786.
[47] H. Seddighi, A.K. Darban, A. Khanchi, J. Fasihi, J. Koleini, LDH(Mg/Al:2)@montmorillonite nanocomposite as a novel anion-exchanger to adsorb uranyl ion from carbonate-containing solutions, J. Radioanal. Nucl. Chem., 314 (2017) 415–427.
[48] P.M. Nekhunguni, N.T. Tavengwa, H. Tutu, Sorption of uranium(VI) onto hydrous ferric oxide-modified zeolite: assessment of the effect of pH, contact time, temperature, selected cations and anions on sorbent interactions, J. Environ. Manage., 204 (2017) 571–582.
[49] H.R. Shakur, R.E. Saraee, M.R. Abdi, G. Azimi, Selective removal of uranium ions from contaminated waters using modified-X nanozeolite, Appl. Radiat. Isot., 118 (2016) 43–55.
[50] L.M. Camacho, S. Deng, R.R., Uranium removal from groundwater by natural clinoptilolite zeolite: effects of pH and initial feed concentration, J. Hazard. Mater., 175 (2010) 393–398.
[51] Y. Arai, M. McBeath, J.R. Bargar, J. Joye, J.A. Davis, Uranyl adsorption and surface speciation at the imogolite–water interface: self-consistent spectroscopic and surface complexation models, Geochim. Cosmochim. Acta, 70 (2006) 2492–2509.
[52] M.M. Hamed, H.E. Rizk, I.M. Ahmed, Adsorption behavior of zirconium and molybdenum from nitric acid medium using low-cost adsorbent, J. Mol. Liq., 249 (2018) 361–370.
[53] M.M. Hamed, M. Holiel, Y.F. El-Aryan, Removal of selenium and iodine radionuclides from waste solutions using synthetic inorganic ion exchanger, J. Mol. Liq., 242 (2017) 722–731.
[54] W. Cheng, C. Ding, Q. Wu, X. Wang, Y. Sun, W. Shi, T. Hayat, A. Alsaedi, Z. Chai, XK. Wang, Mutual effect of U(VI) and Sr(II) on graphene oxides: evidence from EXAFS and theoretical calculations, Environ. Sci. Nano, 4 (2017) 1124–1131.
[55] Y. Sun, X. Wang, Y. Ai, Z. Yu, W. Huang, C. Chen, T. Hayat, A. Alsaedi, XK. Wang, Interaction of sulfonated graphene oxide with U(VI) studied by spectroscopic analysis and theoretical calculations, Chem. Eng. J., 310 (2017) 292–299.
[56] P. Wang, L. Yin, J. Wang, C. Xu, Y. Liang, W. Yao, X. Wang, S. Yu, J. Chen, Y. Sun, XK. Wang, Superior immobilization of U(VI) and ^{243}Am(III) on polyethyleneimine modified lamellar carbon nitride composite from water environment, Chem. Eng. J., 326 (2017) 863–874.
[57] Y. Zou, Y. Liu, X. Wang, G. Sheng, S. Wang, Y. Ai, Y. Ji, Y. Liu, T. Hayat, XK. Wang, Glycerol-modified binary layered double hydroxide nanocomposites for uranium immobilization via extended X-ray absorption fine structure technique and density functional theory calculation, ACS Sustainable Chem. Eng., 5 (2017) 3583–3595.
[58] L. Yin, P. Wang, T. Wen, S. Yu, X. Wang, T. Hayat, A. Alsaedi, XK. Wang, Synthesis of layered titanate nanowires at low temperature and their application in efficient removal of U(VI), Environ. Pollut., 226 (2017) 125–134.
[59] P. Misaelides, D. Fellhauer, X. Gaona, M. Altmaier, H. Geckeis, Thorium(IV) and neptunium(V) uptake from carbonate

containing aqueous solutions by HDTMA-modified natural zeolites, J. Radioanal. Nucl. Chem., 311 (2017) 1665–1671.
[60] Z. Chen, Y. Liang, D.S. Jia, W.Y. Chen, Z.M. Cui, XK. Wang, Layered silicate RUB-15 for efficient removal of UO_2^{2+} and heavy metal ions by ion-exchange, Environ. Sci. Nano, 4 (2017) 1851–1858.
[61] M. Majdan, S. Pikus, A. Gajowiak, A. Gładysz-łaska, H. Krzyzanowska, J. Zuk, M. Bujacka, Characterization of uranium(VI) sorption by organobentonite, Appl. Surf. Sci., 256 (2010) 5416–5421.
[62] M. Galamboš, J. Kufčáková, O. Rosskopfová, P. Rajec, Adsorption of cesium and strontium on natrified bentonites, J. Radioanal. Nucl. Chem., 283 (2010) 803–813.
[63] A. Krajňák, M. Galamboš, O. Rosskopfová, E. Viglašová, P. Rajec, European Nuclear Conference ENC 2012, Young Generation Transaction, Manchester, UK, 2012, pp. 135–141.
[64] M. Galamboš, A. Krajňák, O. Rosskopfová, E. Viglašová, R. Adamcová, P. Rajec, Adsorption equilibrium and kinetic studies of strontium on Mg-bentonite, Fe-bentonite and illite/smectite, J. Radioanal. Nucl. Chem., 298 (2013) 1031–1040.
[65] A. Krajňák, E. Viglašová, M. Galamboš, L. Krivosudský, Application of HDTMA-intercalated bentonites in water waste treatment for U(VI) removal, J. Radioanal. Nucl. Chem., 314 (2017) 2489–2499.
[66] G. Christidis, P.W. Scott, The origin and control of colour of white bentonites from the Aegean islands of Milos and Kimolos, Greece, Miner. Deposita, 32 (1997) 271–279.
[67] A. Filippidis, N. Kantiranis, M. Stamatakis, A. Drakoulis, E. Tzamos, The cation exchange capacity of the Greek zeolitic rocks, Bull. Geol. Soc. Greece, 40 (2007) 723–735.
[68] S.B. Sawin, Analytical use of Arsenazo III, Talanta, 8 (1961) 973–985.
[69] H.E. Hongping, L.F. Ray, Z. Jianxi, Infrared study of $HDTMA^+$ intercalated montmorillonite, Spectrochim. Acta, Part A, 60 (2004) 2853–2859.
[70] G.A. Ikhtiyarova, A.S. Özcan, O. Gök, A. Özcan, Characterization of natural- and organo-bentonite by XRD, SEM, FT-IR and thermal analysis techniques and its adsorption behaviour in aqueous solutions, Clay Miner., 47 (2012) 31–44.
[71] B. Ersoy, E. Ssabah, Ü. Mart, Sorption of Nonionic Organic Contaminants by Organo-Zeolite, 18th International Mining Congress and Exhibition of Turkey - IMCET 2003, ISBN: 975-395-605-3.
[72] V. Swarnkar, R. Tomar, Sorption of chromate by surfactant modified willhendersonite, Acta Chim. Pharm. Indica, 3 (2013) 40–51.
[73] N.D. Zahari, N. Othman, A.Z. Mohd Ishak, Effect of zeolite modification via cationic exchange method on mechanical, thermal, and morphological properties of ethylene vinyl acetate/zeolite composites, Adv. Mater. Sci. Eng., 2013 (2013) 9 pages, doi: 10.1155/2013/394656.
[74] C. Moulin, I. Laszak, V. Moulin, Time-resolved laser-induced fluorescence as a unique tool for low-level uranium speciation, Appl. Spectrosc., 52 (1998) 528–535.
[75] S. Kaufhold, R. Dohrmann, D. Koch, G. Houben, The pH of aqueous bentonite suspensions, Clays Clay Miner., 56 (2008) 338–344.
[76] M. Kilic, E. Apaydin-Varol, A.E. Pütün, Adsorptive removal of phenol from aqueous solutions on activated carbon prepared from tobacco residues: equilibrium, kinetics and thermodynamics, J. Hazard. Mater., 189 (2011) 397–403.
[77] I. Langmuir, The constitution and fundamental properties of solids and liquids, J. Am. Chem. Soc., 38 (1916) 2221–2295.
[78] H.M.F. Freundlich, Over the adsorption in solution, J. Phys. Chem., 57 (1906) 385–471.
[79] M.M. Dubinin, L.V. Radushkievich, The equation of the characteristic curve of the activated charcoal, Proc. Acad. Sci. USSR Phys. Chem. Sect., 55 (1947) 331–337.
[80] S. Lagergren, Zur theorie der sogenannten adsorption geloster stoffe, K. Sven. Vetenskapsakad., 98 (1898) 1–39.
[81] Y.S. Ho, G. McKay, Pseudo-second order model for sorption processes, Process Biochem., 34 (1999) 451–465.
[82] J-P. Simonin, On the comparison of pseudo-first order and pseudo-second order rate laws in the modeling of adsorption kinetics, Chem. Eng. J., 300 (2016) 254–263.
[83] A.R. Kul, H. Koyuncu, Adsorption of Pb(II) ions from aqueous solution by native and activated bentonite: kinetic, equilibrium and thermodynamic study, J. Hazard. Mater., 179 (2010) 332–339.